Transactions, SMiRT-24
BEXCO, Busan, Korea - August 20-25, 2017
Division 01-41

EXPERIMENTAL RESEARCH ON THE LOW CYCLE FATIGUE CHARACTERISTICS OF NICKEL BASE WELD AT ROOM TEMPERATURE

Xiao Qingshan[1], Tang Yi[2], Shi Shaobo[3], Chen Yinqiang[4], and Gui Chun[5]

[1] Engineer, Research Institute of Nuclear Power Operation, China
[2] Professor Engineer, Research Institute of Nuclear Power Operation, China
[3] Senior Engineer, Research Institute of Nuclear Power Operation, China
[4] Senior, Research Institute of Nuclear Power Operation, China
[5] Director, Research Institute of Nuclear Power Operation, China

ABSTRACT

Low cycle fatigue experiment of a dissimilar metal weld of steel and Ni-base alloy with different strain amplitudes at room temperature were carried out, then the curve of strain-life and characteristics of cycle response were obtained. Based on the experimental results of cyclic stress-strain hysteresis loop in fatigue progress at different levels of strain amplitudes, the variation laws of the stress amplitudes and cyclic elastic modulus with respected to the fatigue cycle were analyzed. The effect of the static elastic modulus and dynamic elastic modulus on the low cycle fatigue parameters was investigated. The results showed that the specimen of the weld joint during the progress of fatigue exhibited cyclic hardening at the beginning of 10 cycles, and then exhibited cyclic softening until fractured. The cyclic elastic modulus was decreased with increased number of cycles, and then remained almost stable and decreased dramatically near the end of the life. Finally, the fatigue life curve was concluded, which can be recommended as reference when assessing the integrity of Inconel weld. The static elastic modulus and dynamic elastic modulus showed little different effects on the strain amplitude-life curve.

1. INTRODUCTION

The cyclic stress in low cycle fatigue (LCF) is usually caused by the combined effect of pressure, pipe moment and local thermal stress in PWR. These effects are derived from the thermal shock, the hot stratification cycle and heat shock during the operation. The practical structure inevitably contains the weld joint, and then it is necessary to evaluate the fatigue performance and cyclic deformation characteristic of the weld joint [1]. The nickel alloy is widely used to weld dissimilar metal joints in nuclear power plants. It is considered that crack usually initiates and propagates between steel and Ni-base alloy in the structures. Its fatigue property is a key parameter during design and structural integrity assessment, thus the main purpose in this paper is to acquire the Ni-base weld fatigue character under different load conditions.

Reddy [2] investigated the relationships of 316(N) weld metal and 316L (N)/316(N) between LCF properties and temperature. Yang [3] conducted experiment research on the LCF of TC4 titanium alloy sheet and its laser welding joint, the damage curve of the welding joint deviate from that of base metal due to uniform microstructure and welding defects. Benoit [4] studied the LCF properties of 18% Cr ferrite heat resistant steel base and weld joints at 300°C. Li [5] tested the LCF of welded 25Cr2Ni2MoV steel weld joints, and results showed that cracks developed in the weld and in tempered regions of the hear affected zone, weak zone shifted from the weld to tempered regions with decreasing strain. Zhao [6] investigated the low-cycle fatigue properties of linear friction weld joint of TC11 and TC17 titanium

alloys, and results showed that the stress amplitudes and plastic strain amplitudes exhibited cyclic softening characteristics at higher total strain amplitudes (0.8-1.2%), the elastic modulus during the loading and unloading phases remained constant at the lower strain level, which decreased as the strain amplitude and the number of cycles increased. Zhang [7] studied the LCF behaviours of martensitic steel and weld joint with Ni-based weld metal. The results showed that the weld joints fractured in the weld metal parts, and base steel and Ni-based weld metal exhibit cyclic softening and cyclic hardening, respectively.

In this paper, the LCF test for a dissimilar metal weld of steel and Ni-base alloy was carried out at room temperature. The purpose of the experiment was to evaluate the LCF cycling characteristics of weld joint and the variation of elastic modulus at different strain amplitudes.

2. EXPERIMENTAL

2.1. Materials and specimen

The schematic diagram of weld joint is shown in Fig. 1(a). The weld joint consists of several parts of SA508 Cl.3 base metal, buttering Inconel690, cladding, Inconel690 weld and 316LN base metal. The positions of specimens are shown in Fig. 1(b).

The fatigue specimen of weld joint, as shown in Fig. 2, is perpendicular to the longitudinal direction of the weld. LCF tests were carried out according to ASTM E606 standard [8], using smooth cylindrical specimen shown in Fig. 2. The parallel section part length of specimen is 25 mm, which contains Inconel690 weld and 316LN base metal. So fracture can equally occur in the two parts. After mechanically polishing, the final surface roughness of the specimen Ra is lower than 0.2μm.

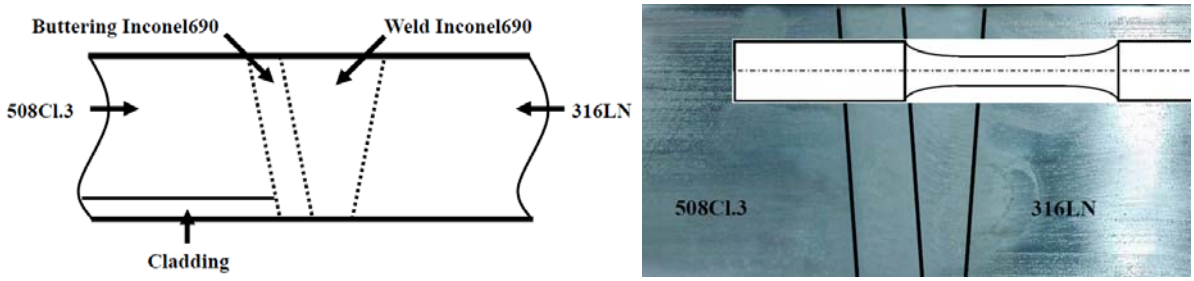

(a) Schematic of the weld joint. (b)Positions of specimens.

Figure 1. Weld joint and specimens

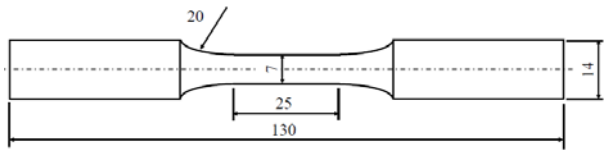

Figure 2. Dimension of fatigue specimen.

2.2. Experimental procedure

The LCF tests were performed in servo-hydraulic machine MTS Landmark 370.10, which has a capacity of ±50kN and a 25mm gage length uniaxial extensometer used for the measurement of strain in the gage section of the specimen. Then the fatigue tests were carried by strain control at room temperature. A triangular waveform was selected with frequency of 0.5 Hz and strain ratio of R_ε=-1, mean strain ε_m=0. In this experiment five different strain amplitudes of 0.2%, 0.3%, 0.4%, 0.5% and 0.6% were chosen. Three

specimens were tested at each level of strain amplitude in order to reduce test error. The fatigue life N_f is defined as the number of cycles for 25% decrease of the maximum tensile stress.

The stress-strain hysteresis loop and wave form are shown in Fig. 3, $\Delta\varepsilon_t$ is the total strain range, $\Delta\varepsilon_e$ is the elastic strain range, $\Delta\varepsilon_p$ is the plastic strain range, $\Delta\sigma$ is the stress range, E_T is the modulus for unloading following a peak tensile stress and E_C is the modulus for loading following a peak compression stress.

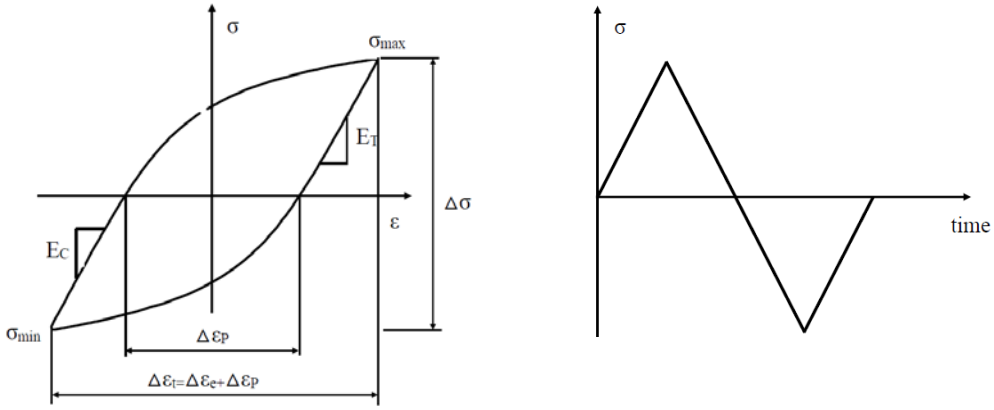

(a) Stress-strain hysteresis loop (b) waveform

Figure 3. Definitions of tension and compression modulus.

Fig. 4 shows the experimental results of weld joint, where ε-N curve shows the variations of fatigue life N_f with the total strain amplitude ε_{ta} in Fig. 5(a), and σ-N curve shows the variations of fatigue life N_f with the mid-life stress amplitudes ε_{ta} in Fig. 5(b).

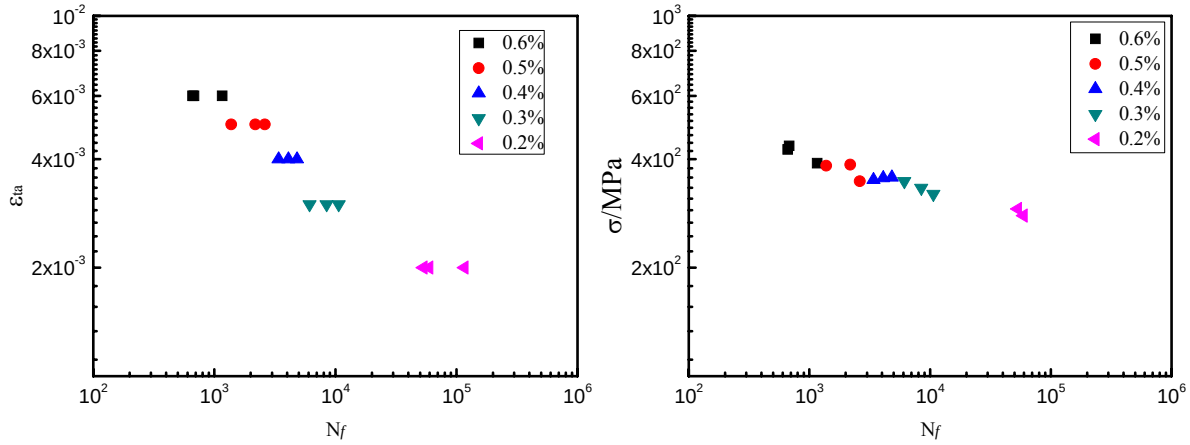

(a) ε-N (b) σ-N

Figure 4. Experimental results of weld joint.

3. RESULTS AND DISCUSSION

3.1. Hysteresis loop

Fig. 5 shows the hysteresis loops of the specimens for five strain amplitudes. At each level of strain amplitude, one representative specimen was selected to describe the relationship between stress and strain.

The hysteresis loops represent the response of material microstructure due to cyclic load, and they are basically symmetrical during loading and unloading. It can be seen that the weld joint exhibits the characteristics of cyclic hardening in the first several cycles and then cyclic softening until fracture. As the strain amplitude increasing, the hysteresis loop becomes wider and higher gradually, indicating that the effect of plastic deformation and loss of energy caused by cyclic loading are strengthened.

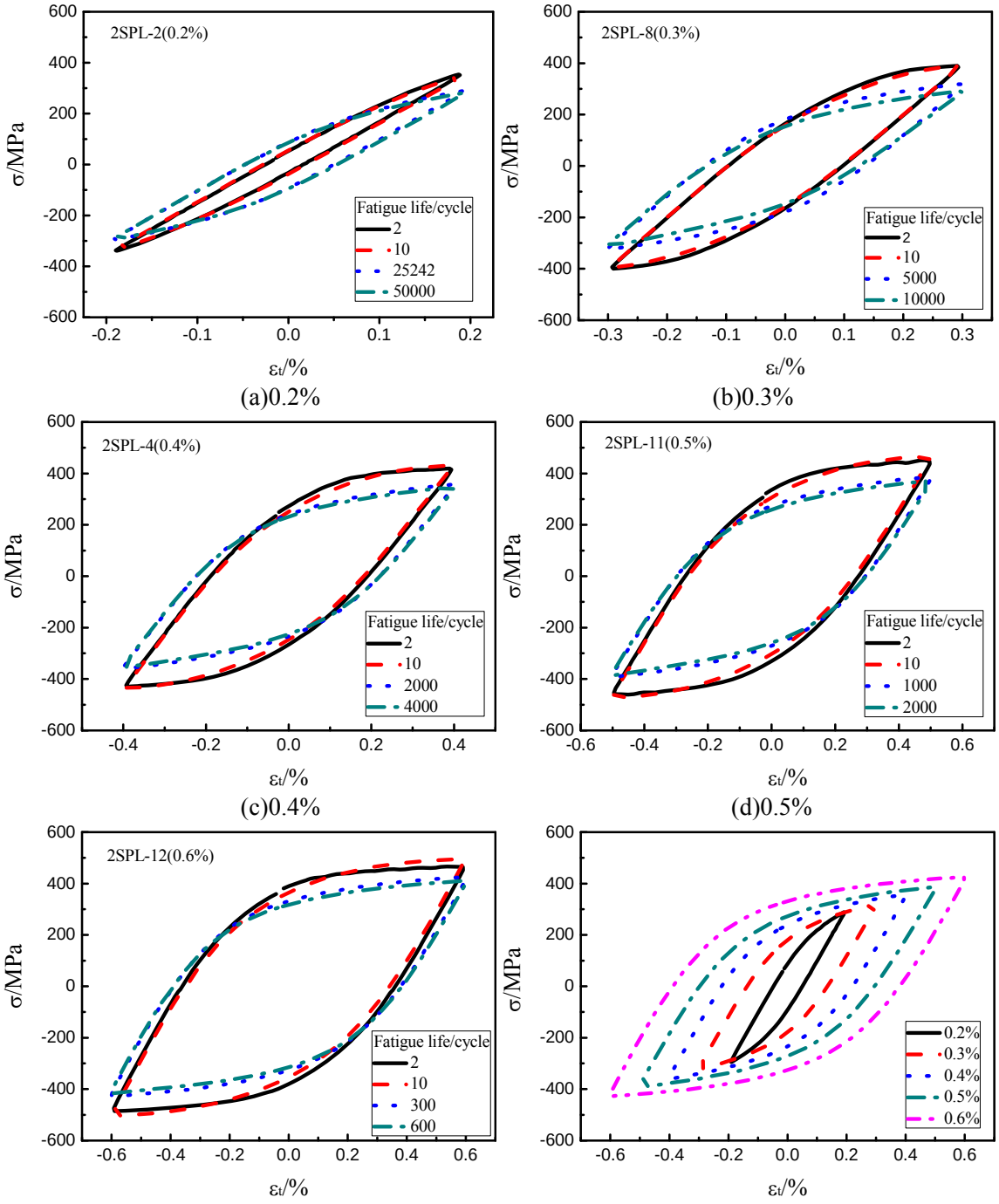

Figure 5. Hysteresis loop of weld joint specimen at different total strain amplitudes.

3.2. Variation of stress amplitude with cycles

Fig. 6 shows the variations of stress amplitude with cycles for weld joint specimen at all levels of strains. And the cyclic responses show the same trend during loading and unloading. When the strain amplitude is $\Delta\varepsilon_t/2$=0.2%, the stress amplitude increases firstly and then decreases with the increasing number of cycles. Then the cyclic softening is followed and its rate of descent is gradually reduced. With increasing of strain amplitude, the cyclic hardening and cyclic softening become much more evident. It shows cyclic hardening in the initial 10 cycles and followed cyclic softening until fracture at strain amplitudes of 0.2% to 0.6%. All of the curves do not show stable cyclic stress amplitude. As the strain amplitude increases, the degree of both cyclic hardening and cyclic softening are increasing.

It was found that the cyclic softening after hardening in the initial stage for some material was significantly concerned with the irregularity of microstructure and material plastic [9]. Thereinto, the irregularity will increase frictional resistance when grains slip in the initial stage, subsequently the plasticity gradually consumed, then the micro crack developed and propagated during the softening stage until fracture.

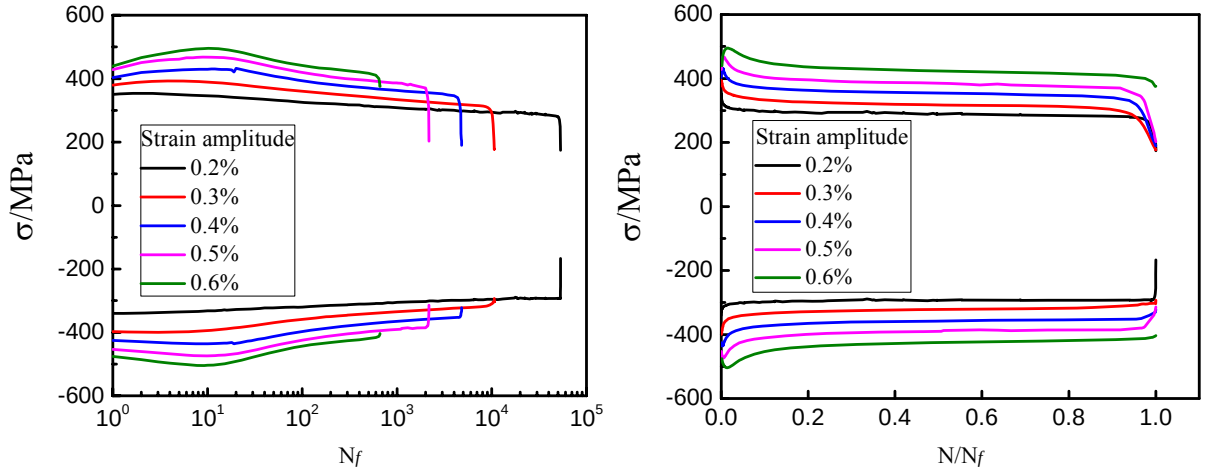

(a) Stress-life in logarithmic coordinate (b) Normalized number of cycles

Figure 6. Variation of stress with the number of cycles at different total strain amplitudes

3.3. Variation of elastic modulus during cyclic deformation

The variation of cyclic elastic modulus with number of cycles at each level of strain is shown in Fig. 7, where the cyclic elastic modulus E^* is the average value of E_T and E_C. It can be seen that the cyclic elastic modulus is larger in the initial stage of fatigue test, and then begins to decline with increase of number of cycles. After 10% of total fatigue life N_f, the degree of decline is becoming slowly and steady until 90% of N_f. It decreased dramatically in the last stage 10% of N_f to the failure. And the cyclic elastic modulus decreases with the increase of the total strain amplitude from 0.2% to 0.5%, and the change of the elastic modulus is not significant when the strain amplitude increases from 0.5% to 0.6%.

Therefore, it can be seen from Fig. 7 that the cyclic elastic modulus decreases with increasing of number of cycles, indicating that the micro cracks formed and developed into small cracks, and this stage is considered as crack initiation. After that, the sharply decreasing of elastic modulus indicates that the crack begin to propagate until fracture. For the material exhibiting cyclic softening response, the point at which the cyclic elastic modulus begin to decrease sharply is considered to be the dividing point between fatigue crack initiation and growth [10-12]. The decreases of stress and elastic modulus before this point are due

to the softening of the material, while the decreases after this point are due to macroscopic crack propagates.

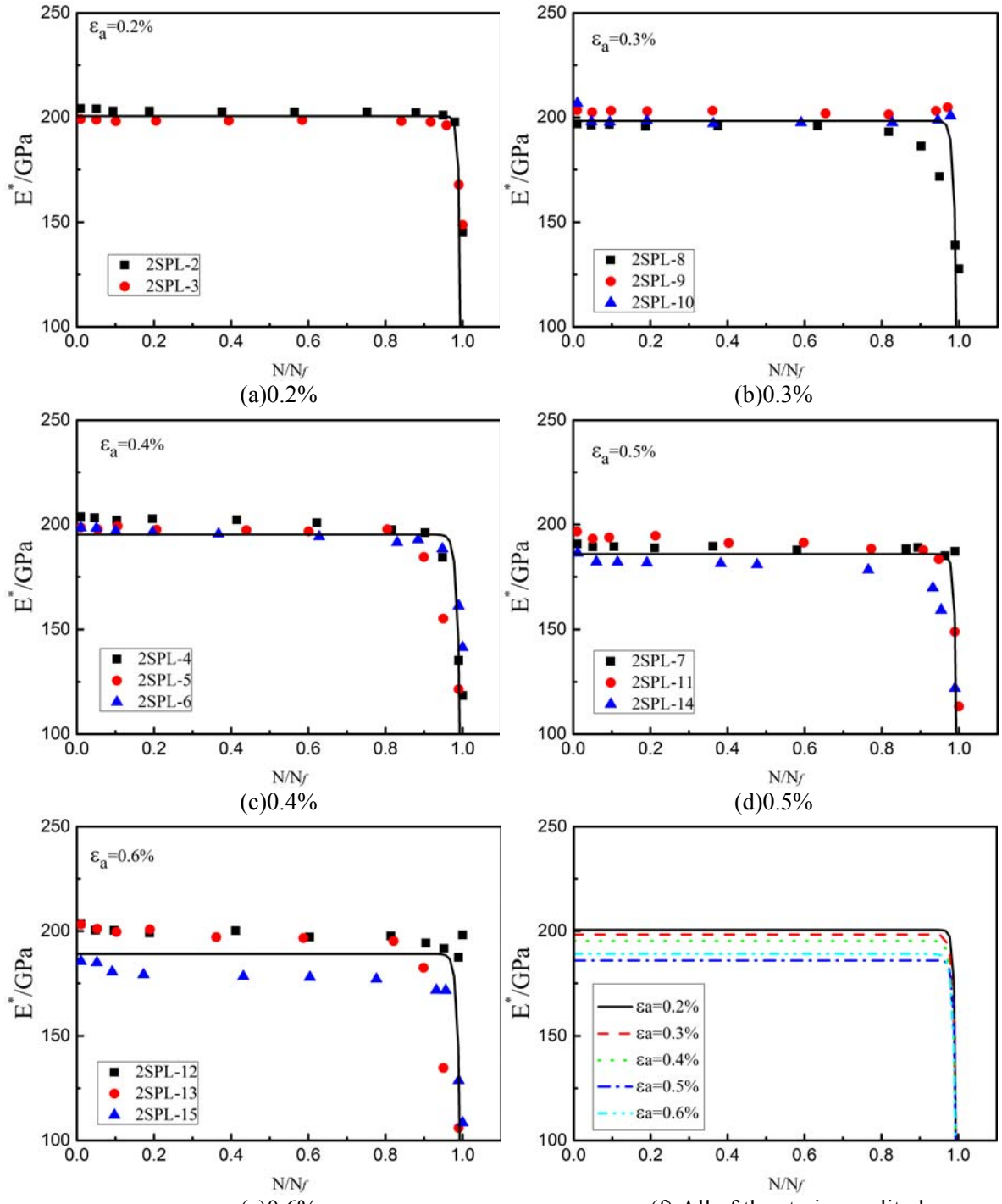

Figure 7. Variation of cyclic elastic modulus with the number of cycles at different total strain amplitudes

3.4. Fatigue life

Then the relationship between stress and total strain can be described by the followings:

$$\frac{\Delta\varepsilon_t}{2}=\frac{\Delta\varepsilon_e}{2}+\frac{\Delta\varepsilon_p}{2}=\frac{\Delta\sigma/2}{E}+\left(\frac{\Delta\sigma/2}{K'}\right)^{1/n'} \tag{1}$$

where K' is the cyclic strength coefficient, n' is the cyclic strain-hardening exponent.

The following Basquin's equation [13-14] is used to evaluate the elastic strain component of fatigue data:

$$\frac{\Delta\varepsilon_e}{2}=\frac{\sigma'_f}{E}\left(2N_f\right)^b \tag{2}$$

where σ'_f is the fatigue strength coefficient, b is the fatigue strength exponent and E is the elastic modulus.

The following Manson-Coffin [15] relationship is used to evaluate the plastic strain component of fatigue data:

$$\frac{\Delta\varepsilon_p}{2}=\varepsilon'_f\left(2N_f\right)^c \tag{3}$$

where ε'_f is the fatigue ductility coefficient, c is the fatigue ductility exponent. Then the relationship between total strain and fatigue life could be defined as:

$$\frac{\Delta\varepsilon_p}{2}=\frac{\Delta\varepsilon_e}{2}+\frac{\Delta\varepsilon_p}{2}=\frac{\sigma'_f}{E}\left(2N_f\right)^b+\varepsilon'_f\left(2N_f\right)^c \tag{4}$$

It can be seen from the equations mentioned above that the calculation accuracy of elastic strain and plastic strain in LCF depends on whether the static elastic modulus or dynamic elastic modulus is selected. Then the static elastic modulus E_0 from static tensile test, the modulus $E_{1/4}$ from first quarter of cyclic loading and cyclic modulus E^* from middle life cycle are chosen to evaluate the elastic strain.

Fig. 8(a) shows the effect of modulus of strain-life curve with three different moduli. It can be seen that Mason-Coffin curve obtained by using static elastic modulus E_0 is at the bottom, while the curve obtained by the modulus $E_{1/4}$ is at the top. When $N_f<10^4$ cycles, the curves obtained by using E^* and $E_{1/4}$ are approximately coincident. When $N_f>10^4$ cycles, the curve obtained by using E^* is approaching the curve obtained by using E_0.

Fig. 8(b) shows the strain amplitude-life curves obtained by cyclic modulus. The intersection of elastic and plastic curves represents the transition fatigue life which is N_f=6500 for this weld joint. When N_f <6500, the plastic strain is dominant and the fatigue resistance is controlled by the ductility. While N_f>6500, the elastic strain is dominant and the fatigue resistance is controlled by the strength.

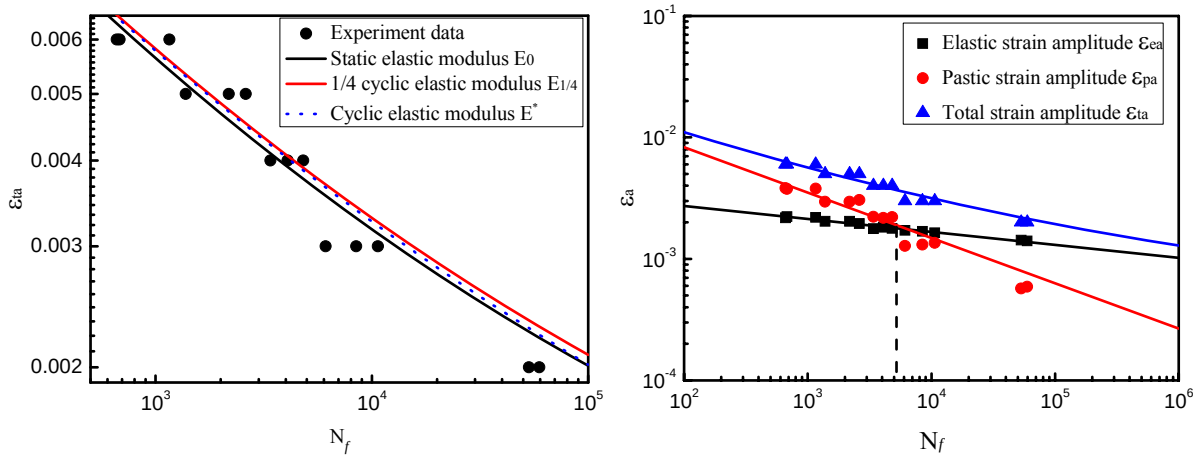

(a) Effect of elastic modulus on strain-life curve (b) Strain amplitude-life curve

Figure 8. Strain-life curves.

3.5. Fracture morphology

As shown in Fig. 9, the weld joint was fractured in the parallel section and located in 316LN steel base, and fracture surface was perpendicular to the axial of specimen from SEM photograph. Fig. 10 shows the fracture surface of fatigued specimen for 2SPL-12 at the strain amplitude of 0.6%. The macroscopic fracture is shown in Fig. 10(a), and it can be clearly seen the crack initiation region, crack growth region and final fracture region. The crack traces point to the specimen surface in crack initiation region, and most of the fracture surface is dominated by the crack initiation and growth region. There is a clear boundary between the crack growth region and final fracture region. In the crack initiation region shown in Fig. 10(b), the cracks were initiated and formed at specimen surface. In the crack growth region shown in Fig. 10(c), there are many fatigue striations caused by cyclic stress. In the final fracture region shown in Fig. 10(d), dimples are the main feature here.

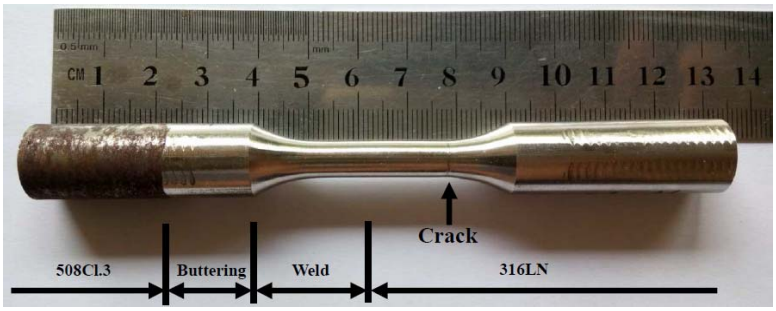

Figure 9. The failure of fatigued specimen.

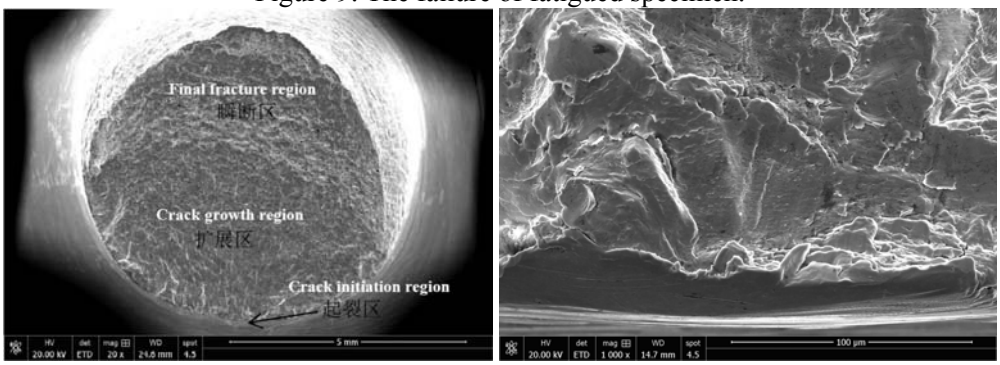

(a) Fracture surface (b)Crack initiation region

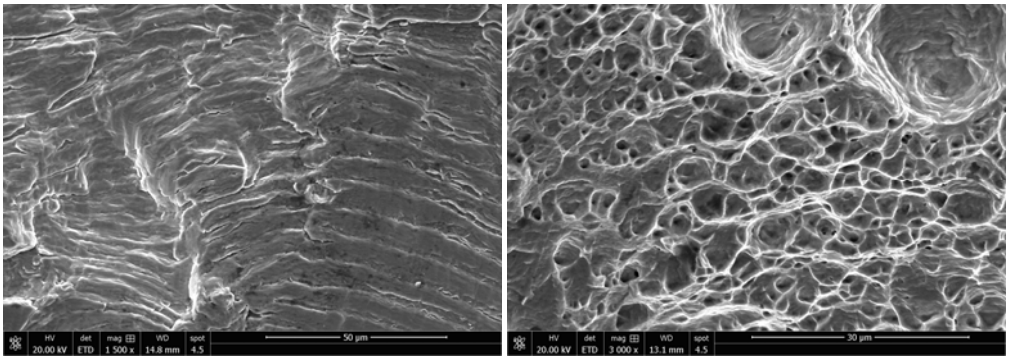

(c) Crack growth region (d) Final fracture region

Figure 10. Fracture morphology.

4. NOMENCLATURE

LCF low cycle fatigue
N_f total fatigue life
N number of cycles
E_T modulus for unloading following a peak tensile stress
E_C modulus for loading following a peak compression stress
E^* cyclic modulus, $E^*=(E_T+E_C)/2$
$\Delta\varepsilon_t$ total strain range
$\Delta\varepsilon_e$ elastic strain range
$\Delta\varepsilon_p$ plastic strain range
σ'_f fatigue strength coefficient
b fatigue strength exponent
ε'_f fatigue ductility coefficient
c fatigue ductility exponent

5. CONCLUSION

The following conclusions can be drawn from the study of LCF for weld joint by stain control at room temperature:
(1)The fracture location of Ni-base dissimilar metal weld happened in stainless steel section, rather than Ni-base alloy weld section.
(2)The weld joint exhibits cyclic hardening during the initial 10 cycles for the strain amplitude of 0.2% to 0.6%, and then exhibits cyclic softening until failure. The larger strain amplitude, the greater degree of cyclic hardening and cyclic softening.
(3)The cyclic elastic modulus decreases slowly in the first 10% of the fatigue lifetime, and then it remains almost stable and decreases rapidly when reaching 90% of the life time. And the larger strain amplitude, the smaller the cyclic elastic modulus. The variation of elastic modulus with fatigue lifetime can clearly characterized the dividing point between fatigue crack initiation and propagation for material with cyclic softening.
(4)The relationship between strain and fatigue life for weld joints could be well characterized using Basquin and Mason-Coffin laws, where the parameters of the fitted curve can be used to predict the LCF life of this weld joint for the strain amplitude of 0.2% to 0.6%. And the static elastic modulus and dynamic elastic modulus have little effect on the strain-life curve of this weld joint.

REFERENCES

[1]Fekete, B., Kasl, J. and Jandova, D. (2015). "Low cycle thermomechanical fatigue of reactor steels: microstructural and fractographic investigations," Mater SciEng, Elsevier, UK , 640 357-374.
[2]Redd, Y., Prasad, G. V., Sandhya, R. and Valsan, M. (2010). "Temperature dependence of low cycle fatigue of 316(N) weld metals and 316L(N)/316(N) weld joints," Materials Science and Technology, Elsevier, UK, 11 1384-1392.
[3]Yang, W. L., Yang, X. H. and Li, X. Y. (2012). "Fatigue damage law of TC4 alloy sheet and laser weld joint," Transactions of Materials and Heat Treatment, China, 23 80-85.
[4]Benoit, A. ,Remy, L. and Koster, A. (2014). "Experimental investigation of the behavior and the low cycle fatigue life of a welded structure," Materials Science and Engineering A, Elsevier, UK, 595 64-76.
[5]Li, Y. F., Cai, Z. P. and Tang, Z. N. (2015). "Weak zone shift in welded joints for low cycle fatigue," J Tsinghua Univ(Sci&Technol), China, 55 1056-1060.
[6]Zhao, P. K., Fu, L. and Chen, H. Y. (2016). "Low cycle fatigue properties of linear friction welded joint of TC11 and TC17 titanium alloys," Jorunal of Alloys and Compounds, Elsevier, UK, 675 248-256.
[7]Zhang, Q. B., Zhang, J. X. and Zhao, P. F. (2016). "Low-cycle fatigue behaviors of a new type of 10% Cr martensitic steel and welded joint with Ni-based weld metal," International Journal of Fatigue, UK, 88 78-87.
[8]ASTM E606 /E606M-12 Standard Test Method for Strain-Controlled Fatigue Testing. (2012). ASTM, West Conshohocken, USA.
[9]Zhao, Y. X., Cai, L. X. and Gao, Q. (2001). "Experimental study on the cyclic deformation behavior of a stainless steel pipe-weld metal under temperature of 240℃," Nuclear Power Engineering, China, 22 138-143.
[10]Tai, J. and Cui, L. (2003). "Mechanical properties of nuclear pressure vessel steel and it's welds," Iron and Steel, China, 38 51-55.
[11]Zhang, G. D., Yu, H. C. and He, Y. H. (2007). "Application research of damage dynamics for low cycle fatigue test," Journal of Aerospace Power, China, 22 1544-1549.
[12]Lv, F. M., Wang, K. and Huang, S. H. (2013). "Experimental research of the high temperature low cycle fatigue charateristics of 12Cr purified steel," Journal of Engineering for Thermal Energy and Power, China, 28 622-627.
[13]Basquin, O. (1910). "The exponential law of endurance tests," Proceedings of the American society for testing and materials, USA, 625-630.
[14]Landgraf, R. W. (1970). "The resistance of metals to cyclic deformation," Achievementof high fatigue resistance in metals and alloys, ASTM STP, Philadelphia, 467 3-36.
[15]Manson, S. S. and Hirschberg, M. H. (1964). "Fatigue behaviour in strain cycling in the low-andintermediate-cycle range," Syracuse University Press, 133-178.